Journal of Thermal Stresses
Publication details, including instructions for authors and subscription information:
http://www.tandfonline.com/loi/uths20

STRESS INTENSITY RELAXATION AT THE TIP OF AN EDGE CRACK IN A FUNCTIONALLY GRADED MATERIAL SUBJECTED TO A THERMAL SHOCK

Zhi-He Jin [a] & R. C. Batra [a]
[a] Department of Engineering Science and Mechanics , Virginia Polytechnic Institute and State University , Blacksburg, Virginia, USA
Published online: 27 Apr 2007.

To cite this article: Zhi-He Jin & R. C. Batra (1996) STRESS INTENSITY RELAXATION AT THE TIP OF AN EDGE CRACK IN A FUNCTIONALLY GRADED MATERIAL SUBJECTED TO A THERMAL SHOCK, Journal of Thermal Stresses, 19:4, 317-339, DOI: 10.1080/01495739608946178

To link to this article: http://dx.doi.org/10.1080/01495739608946178

STRESS INTENSITY RELAXATION AT THE TIP OF AN EDGE CRACK IN A FUNCTIONALLY GRADED MATERIAL SUBJECTED TO A THERMAL SHOCK

Zhi-He Jin and R. C. Batra
Department of Engineering Science and Mechanics
Virginia Polytechnic Institute and State University
Blacksburg, Virginia USA

We analyze thermal stresses and the stress intensity factor in an edge-cracked strip of a functionally graded material (FGM) subjected to sudden cooling at the cracked surface. It is assumed that the shear modulus of the material decreases hyperbolically with the higher value at the surface exposed to the thermal shock and that the thermal conductivity varies exponentially. Volume fractions of the constituents in a ceramic–metal FGM are then determined with the assumed shear modulus gradient using a three-phase model of conventional composites. The differences between the other assumed material properties and those predicted by the three-phase model are delineated and the applicability of the assumed FGM is discussed. It is shown that the maximum tensile thermal stress in the strip without cracks is substantially reduced by the assumed thermal conductivity gradient and that the magnitude of the compressive stress is increased. A strong compressive zone just away from the thermally shocked surface is developed especially at the very initial stage of the thermal shock. Thermal stress intensity factors (TSIF) are numerically calculated based on a singular integral equation derived from the dislocation density along the crack faces. It is shown that while TSIF is relatively insensitive to the shear modulus gradient, it is significantly reduced by the thermal conductivity gradient.

Functionally graded materials for high-temperature applications are special composites usually made from ceramics and metals. The ceramic in a FGM offers thermal barrier effects and protects the metal from corrosion and oxidation. The FGM is toughened and strengthened by the metallic composition. The nonuniform microstructures in materials with continuously graded macroproperties are the most distinctive features of FGMs. The macro-inhomogeneous properties of a FGM reduce thermal stresses when it is subjected to a thermal shock.

Hasselman and coworkers [1, 2] investigated thermal stress reductions in ceramics by spatially changing the thermal conductivity. They studied thermal stresses in solid and hollow cylinders and showed that significant reductions in the magnitude of the tensile thermal stress in the ceramic components could be achieved by appropriately introducing spatial variations of thermal conductivity or porosity, which in turn changed the thermal conductivity and the modulus of

Received 18 September 1995; accepted 15 November 1995.
This work was partially supported by the Office of Naval Research Grant N0014-94-1-1211 with Dr. Y. D. S. Rajapakse as the program manager.
Address correspondence to Professor R. C. Batra, Department of Engineering Science & Mechanics, Virginia Polytechnic Institute and State University, Blacksburg, VA 24061-0219.

Journal of Thermal Stresses, 19:317–339, 1996

0149-5739/96 $12.00 + .00

elasticity. This is evidently related to the concept of a FGM [3]. Noda and Tsuji [4] studied thermal stress reductions in a FGM plate. Tang et al. [5] and Arai et al. [6] considered the optimum design of a FGM for minimizing thermal stresses. By introducing graded ceramic–metal interfaces, thermal residual stresses at the interfaces can also be reduced [7, 8].

The knowledge of crack growth in a FGM is important in order to understand its thermal shock resistance. Kawasaki and Watanabe [9] observed surface crack formation and propagation in a FGM plate when subjected to a thermal shock. Surface cracks in FGM coatings were also observed by Takahashi et al. [10]. It is difficult to develop theoretical models for thermal crack growth in a FGM. Assuming an exponential spatial variation of the elastic modulus, Atkinson and List [11], Dhaliwal and Singh [12], and Delale and Erdogan [13] solved some crack problems for inhomogeneous solids subjected to mechanical loads. By also assuming exponential variations of thermal properties, Jin and Noda [14, 15] and Erdogan and Wu [16] obtained solutions of steady TSIF for inhomogeneous materials. Noda and Jin [17, 18] considered the growth of cracks subjected to a transient thermal loading. The reduction in TSIF can be achieved by appropriately selecting the material parameters [14, 15, 17, 18].

Here we investigate thermal stresses and the change in the stress intensity factor in an edge-cracked strip of a FGM. The aim is to explore the effects of shear modulus and thermal conductivity gradients on thermal stresses and TSIF. It is assumed that the edge-cracked strip of width b, initially at a constant temperature T_0, is suddenly cooled to a temperature T_a on the surface with the crack ($x = 0$) and the other surface ($x = b$) remains at T_0. The shear modulus μ of the material is assumed to be given by $\mu = \mu_0/(1 + \beta x/b)$, where μ_0 is the shear modulus at $x = 0$ and β (≥ 0) is a nondimensional parameter. The thermal conductivity k is assumed to vary according to the relation $k = k_0 e^{\delta x/b}$, where k_0 is the thermal conductivity at $x = 0$ and δ is a nondimensional parameter. The effects of material inhomogeneities on thermal stresses and the stress intensity factor are studied.

A MATERIAL MODEL

FGMs are multiphase materials with spatially varying properties tailored to satisfy specific requirements encountered in engineering applications. The material properties of a FGM, such as Young's modulus and the coefficient of thermal expansion, may be determined from the properties of its constituents and their volume fractions by using an appropriate microthermomechanical model. Conventional composite models may be used when the volume fraction of one constituent is much smaller than that of the other in a two-phase FGM. However, the validity of those models cannot be assured over the entire range of constituent volume fractions because they were developed on the assumption that the constituent distributions and microstructures are uniform in the composite. The main feature of the FGMs is the nonuniform microstructure with the continuous change in constituent volume fractions. In fact, micromechanics models for FGMs are not available [19]. One possibility is to assume a priori properties of a FGM and then

use an appropriate microthermomechanical model to determine the approximate values of the volume fractions of the constituents. The advantages of this method are that the material response can be studied with the assumed variation in properties and the thermomechanical equations are usually simplified. The disadvantage is that the assumed material distributions are usually approximate in the framework of a micromechanical model and may not always result in the desired variations of thermal and mechanical properties.

The thermoelasticity equations for an inhomogeneous solid undergoing plane strain deformations can be written in rectangular Cartesian coordinates as [20]

$$\nabla^2\left(\frac{1-\nu^2}{E}\nabla^2 F\right) - \frac{\partial^2}{\partial y^2}\left(\frac{1}{2\mu}\right)\frac{\partial^2 F}{\partial x^2} - \frac{\partial^2}{\partial x^2}\left(\frac{1}{2\mu}\right)\frac{\partial^2 F}{\partial y^2} + \frac{2\partial^2}{\partial x\,\partial y}\left(\frac{1}{2\mu}\right)\frac{\partial^2 F}{\partial x\,\partial y} + \nabla^2[(1+\nu)\alpha T] = 0 \tag{1}$$

$$\nabla^2 T + \frac{1}{k}\left(\frac{\partial k}{\partial x}\frac{\partial T}{\partial x} + \frac{\partial k}{\partial y}\frac{\partial T}{\partial y}\right) = \frac{1}{\kappa}\frac{\partial T}{\partial t} \tag{2}$$

where F is the Airy stress function, T is the temperature change, ∇^2 is the Laplacian operator, E is Young's modulus, ν is Poisson's ratio, μ is the shear modulus, α is the coefficient of thermal expansion, k is the thermal conductivity, and κ is the thermal diffusivity of the material.

It is extremely difficult to solve Eqs. (1) and (2) analytically for a general spatial variation in material properties. Here we consider a particular FGM. We assume that the mechanical properties are functions of only x and are given by

$$\mu = \frac{\mu_0}{1+\beta(x/b)} \tag{3}$$

$$\frac{E}{1-\nu^2} = \frac{E_0}{1-\nu_0^2}e^{-\gamma(x/b)} \tag{4}$$

where E_0, μ_0, and ν_0 are the Young's modulus, shear modulus, and Poisson's ratio at $x = 0$, respectively; b is a length parameter; and β and γ are constants. Noting that $E = 2(1+\nu)\mu$, the dependence of Young's modulus and the Poisson's ratio upon x can be written as

$$E = E_0\frac{2[1+\beta(x/b)] - (1-\nu_0)e^{\gamma(x/b)}}{(1+\nu_0)[1+\beta(x/b)]^2} \tag{5}$$

$$1-\nu = (1-\nu_0)\frac{e^{\gamma(x/b)}}{1+\beta(x/b)} \tag{6}$$

In Eqs. (3)–(6), β and γ may be determined by

$$\beta = \frac{\mu_0}{\mu_i} - 1 \tag{7}$$

$$\gamma = \ln(1+\beta) + \ln\frac{1-\nu_i}{1-\nu_0} \tag{8}$$

where μ_i and ν_i are the shear modulus and Poisson's ratio at $x = b$, respectively. The Poisson's ratio given by Eq. (6) must satisfy the condition $0 \le \nu \le 0.5$.

The variations in thermal properties are assumed as follows:

$$\alpha = \alpha_p + (\alpha_0 - \alpha_p)e^{\epsilon(x/b)}$$

$$= \alpha_p + (\alpha_0 - \alpha_p)\left(\frac{\alpha_p - \alpha_i}{\alpha_p - \alpha_0}\right)^{(x/b)} \qquad \epsilon = \ln\frac{\alpha_p - \alpha_i}{\alpha_p - \alpha_0} \tag{9}$$

$$k = k_0 e^{\delta(x/b)} \tag{10}$$

$$\kappa = \kappa_0 \tag{11}$$

where α_0, k_0, and κ_0 are the coefficient of thermal expansion (CTE), thermal conductivity and thermal diffusivity at $x = 0$, respectively; α_i is the CTE at $x = b$; α_p is an adjustable constant; and δ is given by

$$\delta = \ln\frac{k_i}{k_0} \tag{12}$$

where k_i is the thermal conductivity at $x = b$.

With assumptions (3)–(12), Eqs. (1) and (2) reduce to the simple forms

$$\frac{1-\nu_0^2}{E_0}\nabla^2(e^{\gamma(x/b)}\nabla^2 F) + \nabla^2[(1+\nu)\alpha T] = 0 \tag{13}$$

$$\nabla^2 T + \frac{\delta}{b}\frac{\partial T}{\partial x} = \frac{1}{\kappa}\frac{\partial T}{\partial t} \tag{14}$$

which may be solved analytically.

Now we determine the volume fractions of the constituents in a two-phase FGM with its mechanical and thermal properties given by Eqs. (3)–(12). We assume that the above particular FGM is obtained by dispersing metallic particulates in a ceramic matrix. The microthermomechanical model used is a *three-phase model* (TPM) or the so-called generalized self-consistent model [21, 22], which is better than other models [19]. Since the volume fraction can generally be deter-

mined with only one assumed property, the other properties predicted by the TPM may be different from those assumed. We will show these differences for an example material. In the TPM, the effective shear modulus, μ, of a composite is given by [22, 23]

$$A\left(\frac{\mu}{\mu_m}\right)^2 + B\left(\frac{\mu}{\mu_m}\right) + C = 0 \tag{15}$$

where μ_m is the shear modulus of the matrix and A, B, and C are dependent on the volume fraction V_i of the metal particulates, the Poisson's ratio of each phase, and the ratio of the shear moduli. We now consider a strip with width b of the assumed FGM; see Figure 1. The strip is subjected to a thermal shock at the surface $x = 0$. It is assumed that the ceramic matrix has a higher shear modulus, $\mu_m > \mu_i$ (subscripts m and i refer to the matrix and particulates, respectively) and the volume fraction V_i of the metallic phase satisfies $V_i = 0$ at $x = 0$ and $V_i = 1$ at $x = b$. (The surface exposed to the thermal shock is completely made of ceramics in FGMs for thermal barrier effect and achieving high corrosion and oxidation resistance). Hence, we have $\mu_0 = \mu_m$ in Eq. (3). Substitution of Eq. (3) into Eq. (15) leads to the following equation for the volume fraction of the metalic phase

$$\frac{A}{[1+\beta(x/b)]^2} + \frac{B}{1+\beta(x/b)} + C = 0 \tag{16}$$

Once the volume fraction is determined, the bulk modulus K of the FGM composite can be obtained from [23]

$$K = K_0 + \frac{V_i(K_i - K_0)}{1 + (1 - V_i)[(K_i - K_0)/(K_0 + 4\mu_0/3)]} \tag{17}$$

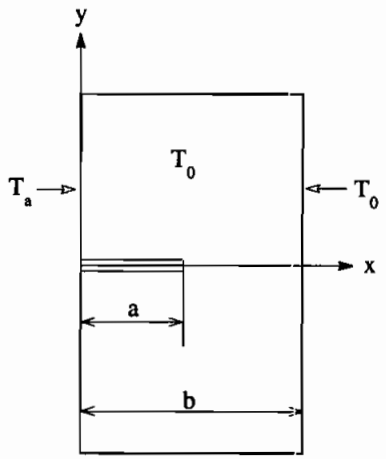

Figure 1. An edge crack in a strip of the FGM subjected to a thermal shock.

where K_0 and K_i are the bulk moduli of the ceramic and the metal, respectively. Then Young's modulus E and Poisson's ratio ν are given by

$$E = \frac{9K\mu}{3K + \mu} \qquad \nu = \frac{E}{2\mu} - 1 \tag{18}$$

The *coefficient of thermal expansion* (CTE) [24, 25] and the thermal conductivity [23, 26] of the composite are given by

$$\alpha = \alpha_i + \frac{\alpha_0 - \alpha_i}{(1/K_0 - 1/K_i)}\left[\frac{1}{K} - \frac{1}{K_i}\right] \tag{19}$$

$$k = k_0\left[1 + \frac{3V_i(k_i - k_0)}{(1 - V_i)(k_i - k_0) + 3k_0}\right] \tag{20}$$

As an example, we consider a FGM with the properties

$$E_i = 200 \text{ GPa} \qquad \nu_i = 1/3 \qquad G_i = 75 \text{ GPa}$$

$$\alpha_i = 15 \times 10^{-6}/°K \qquad k_i = 90\ W/(m°K)$$

for the metal phase and

$$E_0 = 300 \text{ GPa} \qquad \nu_0 = 0.2 \qquad G_0 = 125 \text{ GPa}$$

$$\alpha_0 = 13 \times 10^{-6}/°K \qquad k_0 = 30\ W/(m°K)$$

for the ceramic phase.

Figure 2 shows the shear modulus of the FGM and the volume fraction of the metal phase. Since the volume fraction is determined with the assumed shear modulus, the shear modulus predicted by the TPM is identical to that assumed, Eq. (3). The computed Young's modulus and Poisson's ratio of the TPM are depicted in Figures 3 and 4; these agree well with those obtained from Eqs. (5) and (6). In addition, it can be seen from Figure 4 that the assumed Poisson's ratio satisfies the condition $0 \leq \nu \leq 0.5$. Figure 5 shows the CTE predicted by the microthermomechanical model of Levin [24] and that given by Eq. (9). It is observed that the two CTEs are approximately identical when α_p in Eq. (9) is chosen as $17 \times 10^{-6}/°K$. In general, α_p in Eq. (9) can be chosen by, for example, the least squares method, so that the assumed CTE gives a best approximation to that predicted by a microthermomechanical model. The thermal conductivities obtained from the TPM and the presently assumed one are shown in Figure 6; the difference between them is somewhat large, but the maximum relative error is less than 10%. Here the thermal diffusivity, κ, is not shown. Even if two monophase materials have the same κ, the diffusivity of the mixture of the two materials usually is not a constant

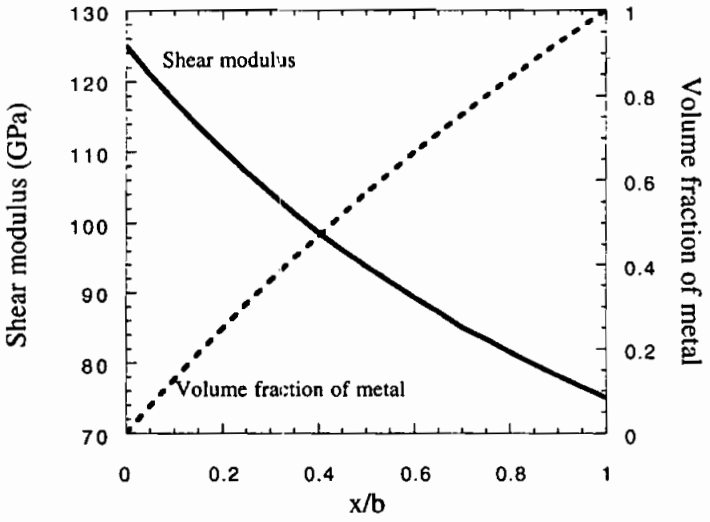

Figure 2. Shear modulus of the FGM and the corresponding volume fraction of the metal in the FGM by the TPM.

since κ depends on the thermal conductivity, density, and specific heat. The present assumption of a constant thermal diffusivity is made for mathematical convenience.

Jin and Mai [27] showed that the difference between Poisson's ratios predicted by the TPM and assumption (6) increases with an increase in β. Hence, with the

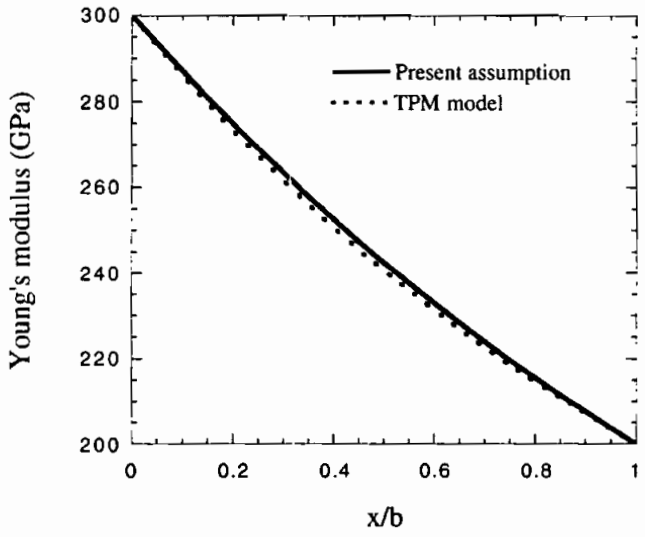

Figure 3. Young's modulus predicted from the TPM and the present assumption, Eq. (5).

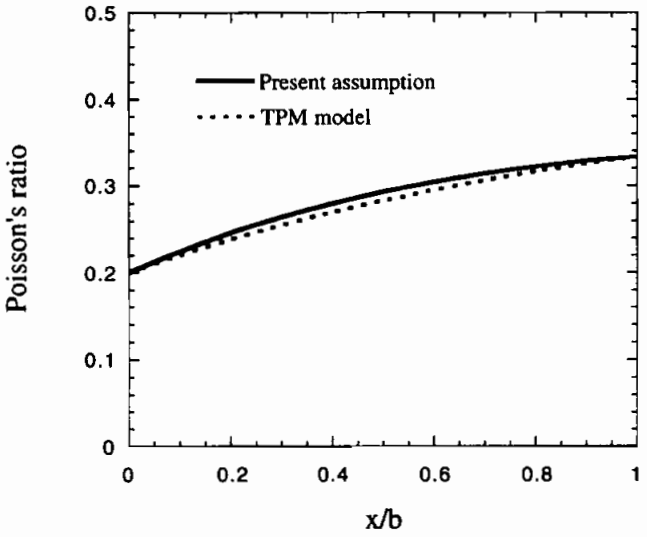

Figure 4. Poisson's ratio predicted from the TPM and the present assumption, Eq. (6).

constituent volume fractions of the TPM based on the shear modulus, the TPM model gives values of the CTE, Young's modulus, Poisson's ratio, and thermal conductivity close to the assumed values when β is not very large. We note that the TPM and other microthermomechanical models developed for macrohomogeneous composites are only approximately valid for FGMs.

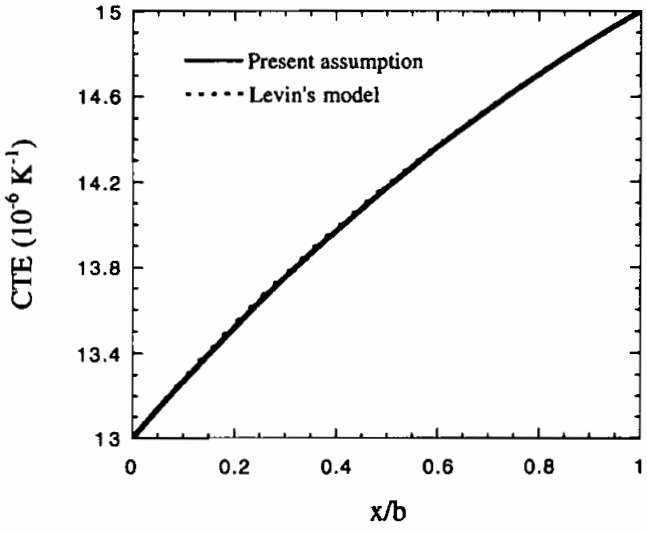

Figure 5. Coefficient of thermal expansion predicted from Levin's model and the present assumption, Eq. (9), $\alpha_p = 17 \times 10^{-6}$ °K^{-1}.

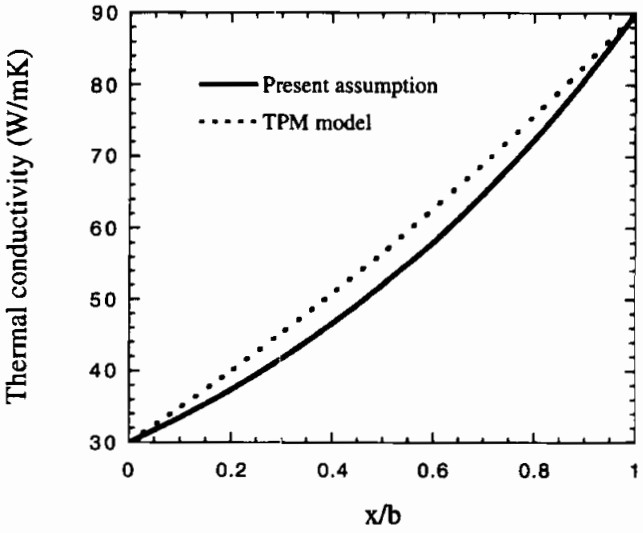

Figure 6. Thermal conductivity predicted from the TPM and the present assumption, Eq. (10).

THERMAL STRESSES

Temperature Field

Consider a long FGM strip of width b with an edge crack of length a as shown in Figure 1. The strip is initially at a constant temperature T_0, and the surface $x = 0$ is suddenly cooled to a temperature T_a. It is assumed that the surface $x = b$ remains at temperature T_0. Hence, the initial and boundary conditions for the temperature field are

$$T(x,t) = T_0 \qquad t = 0 \tag{21}$$

$$T(0,t) = T_a \qquad T(b,t) = T_0 \tag{22a,b}$$

Equations (14), (21), and (22) have the solution

$$\frac{T(x^*,\tau) - T_0}{\Delta T} = \frac{e^{-\delta} - e^{-\delta x^*}}{1 - e^{-\delta}} + \sum_{n=1}^{\infty} B_n e^{-\delta x^*/2} \sin(n\pi x^*) e^{-(n^2\pi^2 + \delta^2/4)\tau} \tag{23}$$

where $x^* = x/b$, $\Delta T = T_0 - T_a$, $\tau = t\kappa/b^2$ is the nondimensional time or the so-called Fourier number, and B_n is given by

$$B_n = \frac{2n\pi}{1 - e^{-\delta}} \left[\frac{1 - (-1)^n e^{-3\delta/2}}{(3\delta/2)^2 + n^2\pi^2} - \frac{e^{-\delta} - (-1)^n e^{-3\delta/2}}{(\delta/2)^2 + n^2\pi^2} \right] \qquad n = 1,2,\ldots \tag{24}$$

Thermal Stresses

For a known spatially one-dimensional temperature field $T = T(x,t)$ in the strip of Figure 1, we seek a particular solution of Eq. (1) with a one-dimensional variation of material properties. Hence, a particular solution of Eq. (1) has the form $F = F(x,t)$ and the equation is reduced to

$$\frac{d^2}{dx^2}\left(\frac{1-\nu^2}{E}\sigma_y^T\right) + \frac{d^2}{dx^2}[(1+\nu)\alpha T] = 0 \tag{25}$$

where

$$\sigma_y^T = \frac{d^2F}{dx^2} \tag{26}$$

The general solution of Eq. (25) is

$$\frac{1-\nu^2}{E}\sigma_y^T = -(1+\nu)\alpha T + Px + Q \tag{27}$$

where P and Q are integration constants to be determined from conditions

$$\int_0^b \sigma_y^I\, dx = 0 \qquad \int_0^b \sigma_y^T x\, dx = 0 \tag{28}$$

which imply that the resultant force and moment in the strip are zero. By substituting Eq. (27) into Eq. (28), P and Q can be determined and the longitudinal stress can be written as

$$\sigma_y^T(x,t) = -\frac{E\alpha T(x,t)}{1-\nu} + \frac{E}{(1-\nu^2)A_0}\left[(A_{22}-xA_{21})\int_0^b \frac{E\alpha T(x,t)}{1-\nu}\,dx - (A_{12}-xA_{11})\int_0^b \frac{E\alpha T(x,t)}{1-\nu}x\,dx\right] \tag{29}$$

where A_{ij} $(i,j=1,2)$ and A_0 are given by

$$A_{11} = \int_0^b E'\,dx \qquad A_{22} = \int_0^b E'x^2\,dx \tag{30a,b}$$

$$A_{12} = A_{21} = \int_0^b E'x\,dx \tag{30c,d}$$

$$A_0 = A_{11}A_{22} - A_{12}A_{21} \tag{30e}$$

with

$$E' = \frac{E}{1-\nu^2} \tag{31}$$

By substituting Eq. (23) into Eq. (29) and noting expressions (5) and (6) for E and ν, we obtain the expression for the thermal stress as

$$\frac{(1-\nu_0)\sigma_y^T(x^*,\tau)}{E_0\alpha_0\Delta T}$$

$$= -\frac{1}{1+\nu_0}\left(2e^{-\gamma x^*} - \frac{1-\nu_0}{1+\beta x^*}\right)\frac{e^{-\delta}-e^{-\delta x^*}}{1-e^{-\delta}}\left[\frac{\alpha_p}{\alpha_0} + \left(1-\frac{\alpha_p}{\alpha_0}\right)e^{\epsilon x^*}\right]$$

$$+ \frac{e^{-\gamma x^*}}{(1+\nu_0)a_0}\left\{(\gamma a_{22} - \gamma^2 a_{12}x^*)\sum_{i=1}^{4}\left[\left(1-\frac{\alpha_p}{\alpha_0}\right)I_{1i} + \frac{\alpha_p}{\alpha_0}I'_{1i}\right]\right.$$

$$\left. -(\gamma^2 a_{12} - \gamma^3 a_{11}x^*)\cdot\sum_{i=1}^{4}\left[\left(1-\frac{\alpha_p}{\alpha_0}\right)I_{2i} + \frac{\alpha_p}{\alpha_0}I'_{2i}\right]\right\}$$

$$+ \frac{1}{1+\nu_0}\sum_{n=1}^{\infty} B_n e^{-(n^2\pi^2+\delta^2/4)\tau}$$

$$\cdot\left\{-\left(2e^{-\gamma x^*} - \frac{1-\nu_0}{1+\beta x^*}\right)e^{-\delta x^*/2}\sin(n\pi x^*)\left[\left(1-\frac{\alpha_p}{\alpha_0}\right)e^{\epsilon x^*} + \frac{\alpha_p}{\alpha_0}\right]\right.$$

$$+ \frac{e^{-\gamma x^*}}{a_0}\left[(\gamma a_{22} - \gamma^2 a_{12}x^*)\left((I_{15}+I_{16})\left(1-\frac{\alpha_p}{\alpha_0}\right) + (I'_{15}+I'_{16})\frac{\alpha_p}{\alpha_0}\right)\right.$$

$$\left.\left. -(\gamma^2 a_{12} - \gamma^3 a_{11}x^*)\left((I_{25}+I_{26})\left(1-\frac{\alpha_p}{\alpha_0}\right) + (I'_{25}+I'_{26})\frac{\alpha_p}{\alpha_0}\right)\right]\right\} \quad (32)$$

where a_0, a_{ij} $(i,j=1,2)$, I_{ij} and I'_{ij} $(i=1,2,\ j=1,\ldots,6)$ are constants given in Appendix A.

THERMAL STRESS INTENSITY FACTOR

The homogeneous solution of Eq. (13) satisfying the symmetry condition at $y=0$ can be expressed as

$$F(x,y) = \frac{1}{\sqrt{2\pi}}\int_{-\infty}^{\infty}\left\{-\frac{\sqrt{(\xi+i\gamma/b)^2}}{|\xi|}e^{-|\xi|y} + e^{-\sqrt{(\xi+i\gamma/b)^2}\,y}\right\}A(\xi)e^{-ix\xi}\,d\xi$$

$$+\sqrt{\frac{2}{\pi}}\int_0^{\infty}\{B_1(\zeta)e^{-\zeta x} + B_2(\zeta)e^{\zeta x}$$

$$+B_3(\zeta)e^{-(\zeta+\gamma/b)x} + B_4(\zeta)e^{(\zeta-\gamma/b)x}\}\cos(y\zeta)\,d\zeta \quad (33)$$

where $A(\xi)$ and $B_i(\zeta)$ $(i=1,2,3,4)$ are unknown functions to be determined. Using the traction free conditions at both surfaces $x=0$ and $x=b$, i.e.,

$$\sigma_x = \sigma_{xy} = 0 \qquad x = 0, b \quad y > 0 \tag{34}$$

four unknowns $B_i(\zeta)$ can be expressed in terms of $A(\xi)$. The stresses can be obtained from the Airy stress function (33) and the displacements are related to the stresses by Hooke's law, i.e.,

$$\frac{\partial u}{\partial x} = \frac{1}{2\mu}\left[\sigma_x - \nu(\sigma_x + \sigma_y)\right] \tag{35a}$$

$$\frac{\partial v}{\partial y} = \frac{1}{2\mu}\left[\sigma_y - \nu(\sigma_x + \sigma_y)\right] \tag{35b}$$

$$\frac{\partial u}{\partial y} + \frac{\partial v}{\partial x} = \frac{\sigma_{xy}}{\mu} \tag{35c}$$

where μ and ν are given by Eqs. (3) and (6).

By introducing the following dislocation density function (e.g., see [29])

$$\phi(x) = \frac{\partial v(x,0)}{\partial x} \tag{36}$$

the longitudinal stress σ_y at the crack line ($y=0$) corresponding to Eq. (33) can be evaluated as

$$\sigma_y = \frac{E_0}{2\pi(1-\nu_0^2)} \int_0^a \left[\frac{1}{x'-x} + k(x,x')\right] \phi(x') e^{-(\gamma/b)x'} \, dx' \tag{37}$$

The superposition of the above stress and that given by Eq. (32) must be zero at the crack face. Hence, the singular integral equation of the crack problem is derived as

$$\int_{-1}^{1} \left[\frac{1}{s-r} + K(r,s)\right] \phi(s) e^{-(a/b)(1+s)\gamma/2} \, ds = -\frac{2\pi(1-\nu_0^2)}{E_0} \sigma_y^T(r,\tau) \qquad |r| \le 1 \tag{38}$$

in which $K(r,s)$ is a Fredholm type kernel given in Appendix B, $r=(2x/a-1)$, and $s=(2x'/a-1)$. According to the singular integral equation method [28–30],

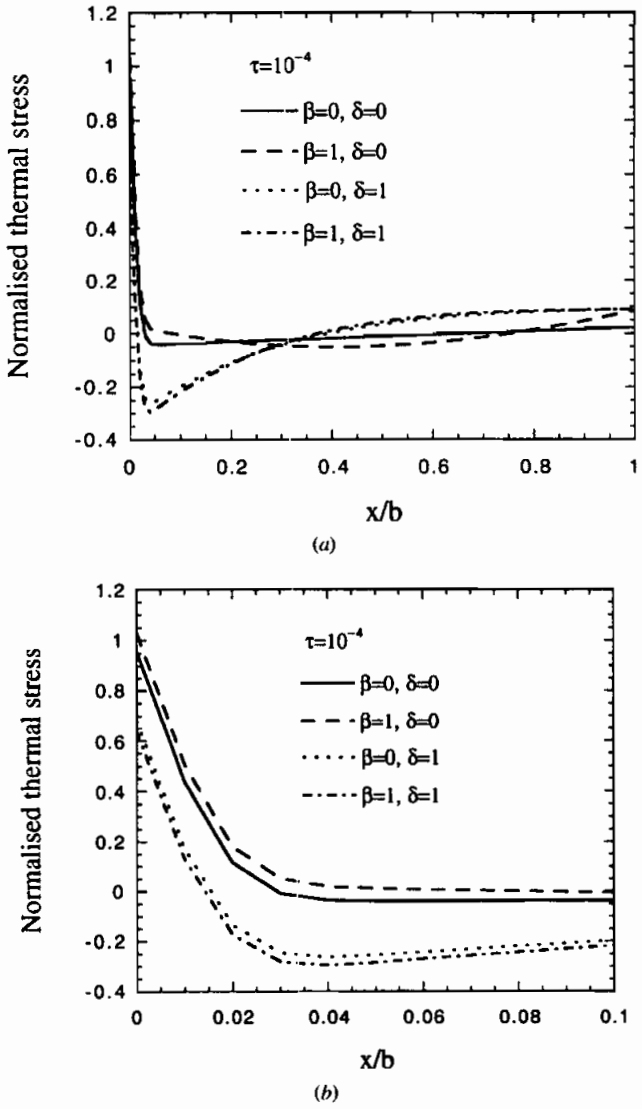

Figure 7. Normalized thermal stress in the FGM strip at (*a*) $\tau = 10^{-4}$, (*b*) $\tau = 10^{-4}$ $(0 \le x/b \le 0.1)$.

Eq. (38) has a solution of the form

$$\phi(r) = e^{(a/b)(1+r)\gamma/2} \frac{\psi(r)}{\sqrt{1-r}} \tag{39}$$

where $\psi(r)$ is a continuous and bounded function on the interval $[-1, 1]$. If $\phi(r)$ is normalized by $(1 + \nu_0)\alpha\Delta T$, then the normalized stress intensity factor, K^*, at the

crack tip is obtained as

$$K^*\left(\frac{a}{b},\tau\right)=\frac{(1-\nu_0)K_I}{E_0\alpha_0\Delta T\sqrt{\pi b}}=-\frac{1}{2}\sqrt{\frac{a}{b}}\,\psi(1,\tau) \tag{40}$$

NUMERICAL RESULTS AND DISCUSSION

It is known that thermal stresses in a material depend not only on the magnitude of the thermal shock but also on the temperature distribution in the material. Thermal stresses will be influenced by the thermal conductivity gradient since it changes the temperature distribution [1, 2]. The main objectives of the present study are to investigate the possible reduction of thermal stresses and the relaxation of thermal stress intensity due to thermal conductivity and elasticity modulus gradients. For simplicity, we assume $\epsilon = 0$ in Eq. (9), i.e., a constant coefficient of thermal expansion. When there is a shear modulus gradient, Poisson's ratio is taken as 0.2 at $x = 0$ (ceramic side) and 0.33 at $x = b$ (metal side).

Effects of Material Inhomogeneities on Thermal Stresses

Figures 7 and 8 show the thermal stress normalized by $E_0\alpha_0\Delta T/(1-\nu_0)$ in the strip free of cracks for various inhomogeneous parameters δ and β at nondimen-

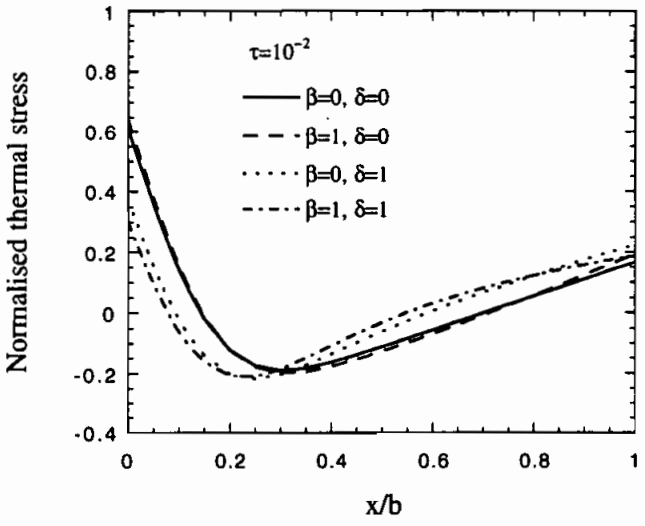

Figure 8. Normalized thermal stress in the FGM strip at $\tau = 10^{-2}$.

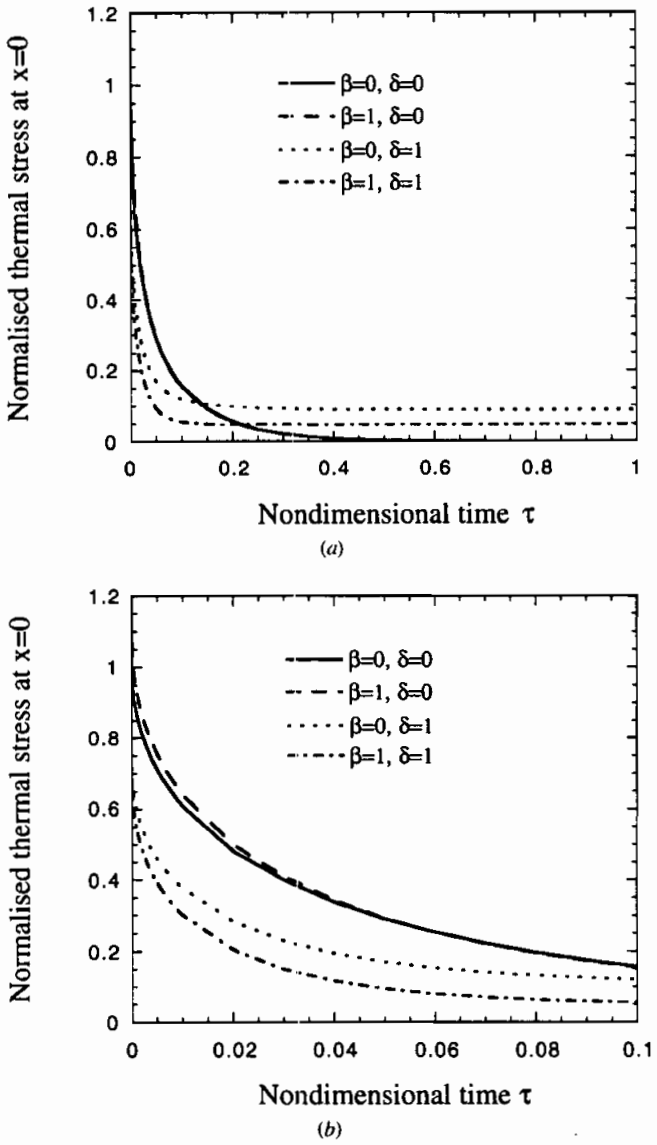

Figure 9. Normalized thermal stress at (*a*) $x = 0$ vs. nondimensional time τ and (*b*) $(0 \leq \tau \leq 0.1)$.

sional times $\tau = 10^{-4}$ and 10^{-2}, respectively. It is seen from Figures 7*a* and 7*b* that at $\tau = 10^{-4}$, the maximum tensile thermal stress occurring at $x = 0$ is significantly reduced by increasing δ, a parameter of thermal conductivity gradient, when there are no gradients of mechanical properties. However, the magnitude of the maximum compressive stress increases with increasing δ. It seems that the thermal stress is relatively insensitive to β, a parameter of shear modulus gradient. The

maximum tensile stress increases slightly with increasing β when the material is thermally homogeneous. The inverse occurs when δ is not zero. For $\beta = 0$ and $\delta = 1$, the maximum tensile stress is only 72% of that in the homogeneous material and drops to 68% of that in the homogeneous material for $\beta = 1$ and $\delta = 1$. It is also observed that high compressive stresses are developed near the surface $x = 0$, which will retard the growth of the crack into the material. Figure 8 shows similar results for $\tau = 10^{-2}$. In Figure 9*a*, the evolution of the normalized tensile stress at $x = 0$ (which is maximum in the strip at a given time) is depicted. The tensile stress decreases with increasing τ and the all-time maximum occurs at $\tau = 0^+$. While the thermal stress in a homogeneous strip vanishes as $\tau \to \infty$, the stress in a nonhomogeneous strip is nonzero. Figure 9*b* highlights the results for the interval $\tau \in [0, 0.1]$.

Effects of Material Inhomogeneities on TSIF

The TSIF can be calculated from Eqs. (39) and (40) after the singular integral equation (38) is numerically solved. The effects of the assumed gradients of material properties on the TSIF are then studied.

For a thermally homogeneous material ($\delta = 0$), the general pattern in the variations of the normalized TSIF, $K^*(a/b, \tau)$, with time and crack length is similar to that in a homogeneous material [31–34]. For fixed values of β and the crack length, the TSIF increases from zero and passes through a peak value at a particular time that increases with the crack length and decreases to zero subsequently. There is a critical normalized crack length (normalized by the width of the strip) l_c ($= a_c/b$) at which the peak value of TSIF reaches a maximum. Figure 10

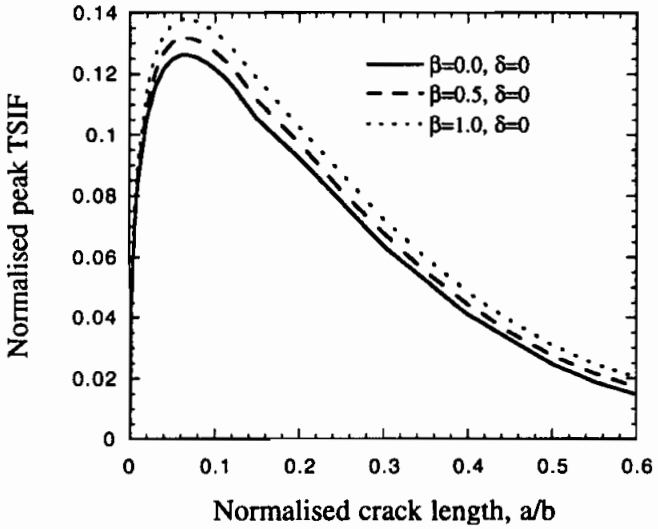

Figure 10. Normalized peak TSIF in the edge-cracked FGM strip ($\delta = 0$; $\beta = 0.5, 1.0$).

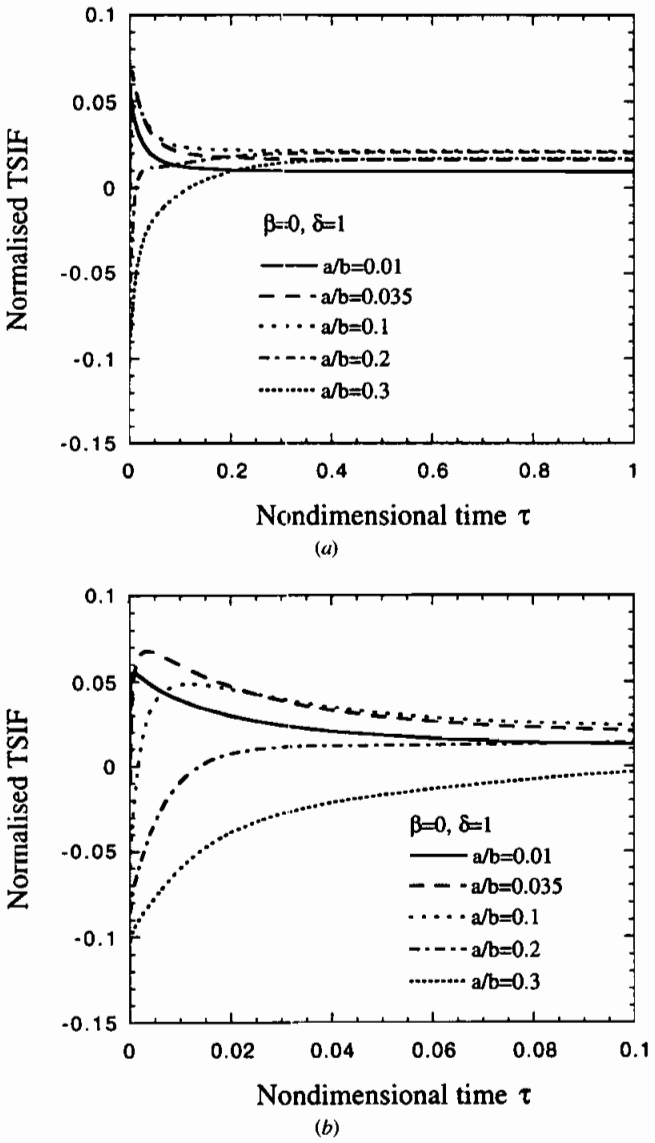

Figure 11. Normalized TSIF versus nondimensional time τ (*a*) for various crack lengths a/b ($\beta = 0$; $\delta = 1$) and (*b*) ($0 \leq \tau \leq 0.1$).

shows the peak TSIF versus the normalized crack length a/b for different values of β. The peak TSIFs in the inhomogeneous material ($\beta \neq 0$) are slightly higher than those in a homogeneous material ($\beta = 0$, with Young's modulus and Poisson's ratio being E_0 and ν_0). The inhomogeneity has a negligible effect on the critical length l_c, which is about 0.065 for the homogeneous material. We have also

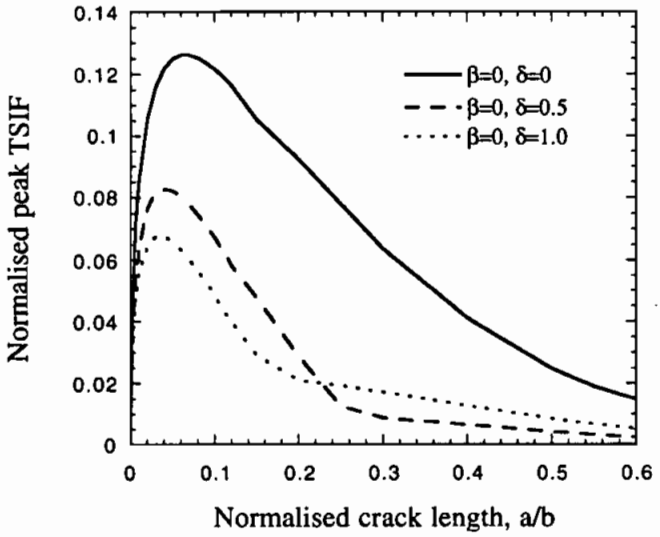

Figure 12. Normalized peak TSIF vs. normalized crack length ($\beta = 0.0$; $\delta = 0.5, 1.0$).

investigated the influence of Poisson's ratio on the TSIF. When Poisson's ratios ν_0 at $x = 0$ and ν_1 at $x = b$ are varied in such a manner that the parameter γ in Eqs. (4)–(6) and (8) remains unchanged, no change in the TSIF is observed. However, if γ becomes smaller due to the variations of ν_0 and ν_1, the TSIF becomes smaller and may be slightly lower than that for the homogeneous material.

For a mechanically homogeneous material ($\beta = 0$ and $\nu_0 = \nu_1$), the pattern in the variations of the TSIF with time and crack length is similar to that of a homogeneous material for short cracks but different for long cracks. Figure 11*a* shows the TSIF versus the nondimensional time τ for various normalized crack lengths a/b for $\delta = 1$. For cracks longer than $a/b = 0.035$, the TSIF is virtually negative at the initial stage of the thermal shock. For cracks longer than $a/b = 0.2$, the TSIF is negative for $\tau < 10^{-2}$ and reaches the peak at the steady state. Figure 11*b* illustrates results for the integral $\tau \in [0, 0.1]$. Physically, a negative TSIF means that no crack growth occurs. Figure 12 shows the normalized peak TSIF as a function of a/b for different δ. The peak TSIF increases with a/b, reaches its maximum at about $a/b = l_c = 0.035$, and then decreases with further increase in a/b. It is seen that the peak TSIFs for the FGM are significantly reduced as compared with that for the homogeneous material. The maximum normalized TSIF is 0.06774 for $\delta = 1$, nearly half of its value 0.1263 for the homogeneous material. Also, the critical crack length $a_c/b = l_c$ at which the peak TSIF has the maximum value is about 0.035 for the FGM, which is much smaller than 0.065, the value for the homogeneous material. Jin and Mai [35] showed that in a homogeneous ceramic, a preexisting crack shorter than $l_c = 0.065$ will grow unstably once initiated by a thermal shock and cause a sudden drop of the residual strength. For the nonhomogeneous material with a thermal conductivity gradient, only cracks

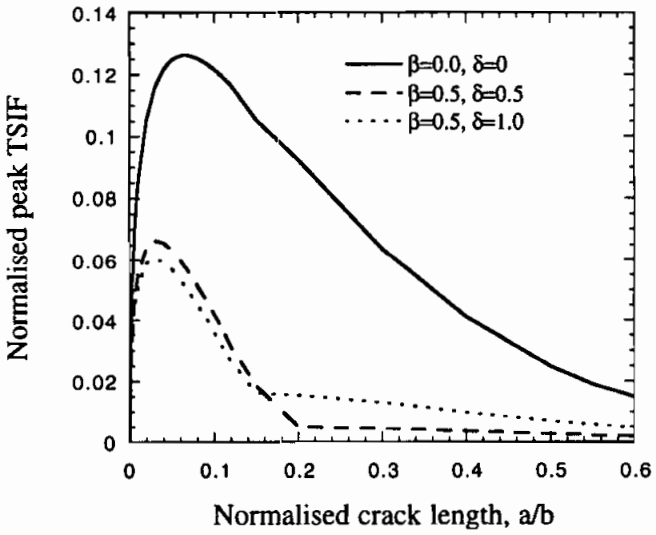

Figure 13. Normalized peak TSIF vs. normalized crack length ($\beta = 0.5$; $\delta = 0.5, 1.0$).

shorter than $l_c = 0.035$ will grow unstably when initiated; i.e., the cracks between $a/b = 0.035$ and 0.065 will no longer cause a sudden drop of the residual strength. Even if a short crack may grow unstably, it will be arrested earlier due to the increasing toughness of the FGM. Figures 13 and 14 show similar results for materials with both mechanical and thermal inhomogeneities (both β and δ are

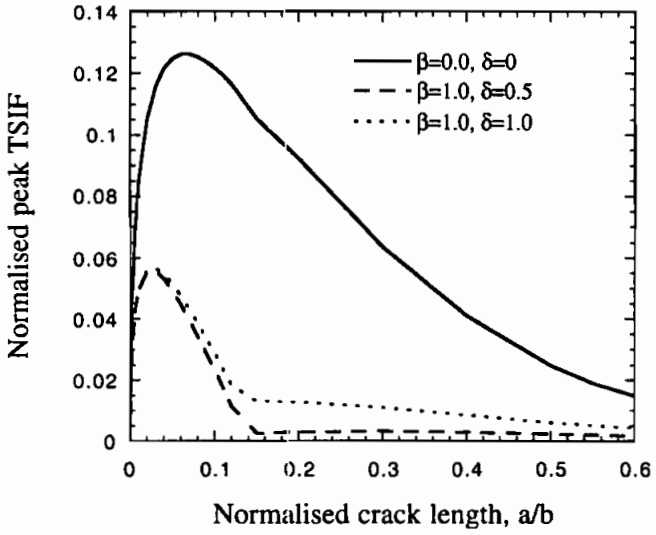

Figure 14. Normalized peak TSIF vs. normalized crack length ($\beta = 1.0$; $\delta = 0.5, 1.0$).

not zero). It is again observed that the maximum TSIF is reduced to about half of that for the homogeneous material. The critical crack length for $\beta = 1$ and $\delta = 1$ is only 0.025.

CONCLUSIONS

A FGM is proposed for improving the thermal shock resistance. The FGM has a hyperbolically decreasing shear modulus with the higher value at the surface exposed to the thermal shock and the thermal conductivity of the FGM increases exponentially. Such a FGM may be obtained by dispersing metal particulates in a ceramic matrix with an appropriate particulate volume fraction gradation. It is shown that the maximum tensile thermal stress in a strip of the FGM is substantially reduced by the assumed thermal conductivity gradient and the peak magnitude of the compressive stress is increased. A strong compressive zone just away from the thermally shocked surface is developed, especially at the initial stage of the thermal shock. The TSIF for an edge crack in the FGM strip is relatively insensitive to the shear modulus gradient but is significantly reduced by the thermal conductivity gradient.

REFERENCES

1. D. P. H. Hasselman and G. E. Youngblood, Enhanced Thermal Stress Resistance of Structural Ceramics with Thermal Conductivity Gradient, *J. Amer. Ceram. Soc.*, vol. 61, pp. 49–52, 1978.
2. K. Satyamurthy, D. P. H. Hasselman, J. P. Singh, and M. P. Kamat, Effect of Spatial Variation of Thermal Conductivity on Magnitude of Tensile Thermal Stresses in Brittle Materials Subjected to Convective Heating, in D. P. H. Hasselman and R. A. Heller (eds.), *Thermal Stresses in Severe Environments*, pp. 325–342, Plenum Press, New York, 1980.
3. M. Koizumi, The Concept of FGM, in J. B. Holt, M. Koizumi, T. Hirai, and Z. A. Munir (eds.), Functionally Gradient Materials, *Ceramic Trans.*, vol. 34, pp. 3–10, American Ceramic Society, Westerville, OH, 1993.
4. N. Noda and T. Tsuji, Steady Thermal Stresses in a Plate of a Functionally Gradient Material, in M. Yamanouchi, M. Koizumi, T. Hirai, and I. Shiota (eds.), *Proc. 1st Int. Symp. on Functionally Gradient Materials*, pp. 339–344, Sendai, Japan, 1990.
5. X. F. Tang, L. M. Zhang, Q. J. Zhang, and R. Z. Yuan, Design and Structural Control of PSZ-Mo Functionally Gradient Materials with Thermal Stress Relaxation, in J. B. Holt, M. Koizumi, T. Hirai, and Z. A. Munir (eds.), Functionally Gradient Materials, *Ceramic Trans.*, vol. 34, pp. 457–463, American Ceramic Society, Westerville, OH, 1993.
6. Y. Arai, H. Kobayashi and T. Tamura, Elastic-Plastic Thermal Stress Analysis for Optimum Design of Functionally Gradient Material, in *Thermal Stress '95, Proc. 1st Int. Symp. on Thermal Stresses and Related Topics*, pp. 355–358, Shizuoka University, Hamamatsu, Japan, June 1995.
7. A. Kawasaki and R. Watanabe, Finite Element Analysis of Thermal Stress of the Metal/Ceramic Multi-Layer Composites with Controlled Compositional Gradients, *J. Japan Inst. Metals*, vol. 51, pp. 525–529, 1987. (in Japanese)
8. J. T. Drake, R. L. Williamson, and B. H. Rabin, Finite Element Analysis of Thermal Residual Stresses at Graded Ceramic-Metal Interfaces, Part II: Interface Optimization for Residual Stress Reduction, *J. Appl. Phys.*, vol. 74, pp. 1321–1326, 1993.

9. A. Kawasaki and R. Watanabe, Fabrication of Disk-Shaped Functionally Gradient Materials by Hot Pressing and Their Thermomechanical Performance, in J. B. Holt, M. Koizumi, T. Hirai, and Z. A. Munir (eds.), Functionally Gradient Materials, *Ceramic Trans.*, vol. 34, pp. 157–164, American Ceramic Society, Westerville, OH, 1993.
10. H. Takahashi, T. Ishikawa, D. Okugawa, and T. Hashida, Laser and Plasma-ARC Thermal Shock/Fatigue Fracture Evaluation Procedure for Functionally Gradient Materials, in G. A. Schneider and G. Petzow (eds.), *Thermal Shock and Thermal Fatigue Behavior of Advanced Ceramics*, pp. 543–554, Kluwer Academic Publ., Dordrecht, 1993.
11. C. Atkinson and R. D. List, Steady State Crack Propagation into Media with Spatially Varying Elastic Properties, *Int. J. Engrg Sci.*, vol. 16, pp. 717–730, 1978.
12. R. S. Dhaliwal and B. M. Singh, On the Theory of Elasticity of a Non-Homogeneous Medium, *J. Elasticity*, vol. 8, pp. 211–219, 1978.
13. F. Delale and F. Erdogan, The Crack Problem for a Nonhomogeneous Plane, *ASME J. Appl. Mech.*, vol. 50, pp. 609–614, 1983.
14. Z.-H. Jin and N. Noda, An Internal Crack Parallel to the Boundary of a Nonhomogeneous Half Plane under Thermal Loading, *Int. J. Engrg Sci.*, vol. 31, pp. 793–806, 1993.
15. N. Noda and Z.-H. Jin, Thermal Stress Intensity Factors for a Crack in a Strip of a Functionally Gradient Material, *Internat. J. Solids Structures*, vol. 30, pp. 1039–1056, 1993.
16. F. Erdogan and B. H. Wu, Analysis of FGM Specimens for Fracture Toughness Testing, in J. B. Holt, K. Koizumi, T. Hirai, and Z. A. Munir (eds.), Functionally Gradient Materials, *Ceramic Trans.*, vol. 34, pp. 39–46, American Ceramic Society, Westerville, OH, 1993.
17. N. Noda and Z.-H. Jin, A Crack in Functionally Gradient Materials Under Thermal Shock, *Arch. Appl. Mech.*, vol. 64, pp. 99–110, 1994.
18. Z.-H. Jin and N. Noda, Transient Thermal Stress Intensity Factors for a Crack in a Semi-Infinite Plane of a Functionally Gradient Material, *Internat. J. Solids Structures*, vol. 31, pp. 203–218, 1994.
19. J. R. Zuiker, Functionally Graded Materials: Choice of Micromechanics Model and Limitations in Property Variation, *Composites Engrg.*, vol. 5, pp. 807–819, 1995.
20. Z.-H. Jin and N. Noda, Crack-Tip Singular Fields in Nonhomogeneous Materials, *ASME J. Appl. Mech.*, vol. 61, pp. 738–740, 1994.
21. J. C. Smith, Simplification of van der Poel's Formula for the Shear Modulus of a Particulate Composite, *J. Research National Bureau of Standards—A. Physics and Chemistry*, vol. 79, pp. 419–423, 1975.
22. R. M. Christensen and K. H. Lo, Solutions for Effective Shear Properties in Three Phase Sphere and Cylinder Models, *J. Mech. Phys. Solids*, vol. 27, pp. 315–330, 1979.
23. R. M. Christensen, *Mechanics of Composite Materials*, John Wiley & Sons, New York, 1979.
24. V. M. Levin, Thermal Expansion Coefficients of Heterogeneous Materials, *Mekh. Tverd. Tela*, vol. 2, pp. 88–94, 1967. (Russian)
25. B. W. Rosen and Z. Hasin, Effective Thermal Expansion Coefficients and Specific Heats of Composite Materials, *Internat. J. Engrg Sci.*, vol. 8, pp. 157–173, 1970.
26. Z. Hashin and S. Shtrikman, A Variational Approach to the Theory of the Effective Magnetic Permeability of Multiphase Materials, *J. Appl. Phys.*, vol. 33, p. 3125, 1962.
27. Z.-H. Jin and Y.-W. Mai, Thermal Fracture of Functionally Gradient Ceramics, 6th Intl. Symp. on Fracture Mechanics of Ceramics, Germany, 1995.
28. N. I. Muskhelishvili, *Singular Integral Equations*, Noordhoff, Groningen, 1953.
29. G. D. Gupta and F. Erdogan, The Problem of Edge Cracks in an Infinite Strip, *ASME J. Appl. Mech.*, vol. 41, pp. 1001–1006, 1974.
30. A. C. Kaya and F. Erdogan, On the Solution of Integral Equations with Strongly Singular Kernels, *Quart. Appl. Math.*, vol. 45, pp. 105–122, 1987.
31. A. F. Emery, G. E. Walker, Jr., and J. A. Williams, A Green's Function for the Stress Intensity Factors of Edge Cracks and Its Application to Thermal Stresses, *ASME J. Basic Engrg.*, vol. 91, pp. 618–624, 1969.
32. H. F. Nied, Thermal Shock Fracture in an Edge-Cracked Plate, *J. Thermal Stresses*, vol. 6, pp. 217–229, 1983.
33. A. E.-F. A. Rizk and S. F. Radwan, Fracture of a Plate Under Transient Thermal Stress, *J. Thermal Stresses*, vol. 16, pp. 79–102, 1993.

34. X. R. Wu, Application of Weight Function Method for Crack Analysis in Thermal Stress Fields, in G. A. Schneider and G. Petzow (eds.), *Thermal Shock and Thermal Fatigue Behaviour of Advanced Ceramics*, pp. 119–141, Kluwer Academic Publ., Dordrecht, 1993.
35. Z.-H. Jin and Y.-W. Mai, Effects of Damage on Thermal Shock Strength Behavior of Ceramics, *J. Amer. Ceram. Soc.*, vol. 78, pp. 1873–1881, 1995.

APPENDIX A

Constants a_0, a_{ij}, I_{ij} and I'_{ij} in Eq. (32)

The constants a_0, a_{ij} $(i,j=1,2)$, I_{ij} and I'_{ij} $(i=1,2,\ j=1,\ldots,6)$ in the thermal stress expression (32) are given as

$$a_{11} = 1 - e^{-\gamma}$$

$$a_{12} = a_{21} = 1 - (1+\gamma)e^{-\gamma}$$

$$a_{22} = 2 - \left[1 + (1+\gamma)^2\right]e^{-\gamma}$$

$$a_0 = 1 - (2+\gamma^2)e^{-\gamma} + e^{-2\gamma}$$

and

$$I_{11} = \frac{2e^{-\delta}}{1-e^{-\delta}} \cdot \frac{1-e^{-(\gamma-\epsilon)}}{\gamma-\epsilon}$$

$$I_{12} = \frac{2}{1-e^{-\delta}} \cdot \frac{e^{-(\gamma+\delta-\epsilon)}-1}{\gamma+\delta-\epsilon}$$

$$I_{13} = -\frac{(1-\nu_0)e^{-\delta}}{1-e^{-\delta}} \int_0^1 \frac{e^{\epsilon x}}{1+\beta x}\,dx$$

$$I_{14} = \frac{1-\nu_0}{1-e^{-\delta}} \int_0^1 \frac{e^{(\epsilon-\delta)x}}{1+\beta x}\,dx$$

$$I_{15} = \frac{2n\pi}{(\gamma+\delta/2-\epsilon)^2 + n^2\pi^2}\left[1-(-1)^n e^{-(\gamma+\delta/2-\epsilon)}\right] \qquad n=1,2,\ldots$$

$$I_{16} = -(1-\nu_0)\int_0^1 \frac{e^{(\epsilon-\delta/2)x}}{1+\beta x}\sin(n\pi x)\,dx \qquad n=1,2\ldots$$

$$I_{21} = \frac{2e^{-\delta}}{(\gamma-\epsilon)(1-e^{-\delta})}\left[\frac{1-e^{-(\gamma-\epsilon)}}{\gamma-\epsilon} - e^{-(\gamma-\epsilon)}\right]$$

$$I_{22} = \frac{2}{(\gamma+\delta-\epsilon)(1-e^{-\delta})}\left[\frac{e^{-(\gamma+\delta-\epsilon)}-1}{\gamma+\delta-\epsilon} + e^{-(\gamma+\delta-\epsilon)}\right]$$

$$I_{23} = -\frac{1}{\beta}\left[I_{13} + \frac{(1-\nu_0)e^{-\delta}}{1-e^{-\delta}} \cdot \frac{e^{\epsilon}-1}{\epsilon}\right]$$

$$I_{24} = \frac{1}{\beta}\left[\frac{1-\nu_0}{1-e^{-\delta}}\frac{e^{\epsilon-\delta}-1}{\epsilon-\delta} - I_{14}\right]$$

$$I_{25} = \frac{2(-1)^n n\pi}{\rho^2}\left[\frac{2(\epsilon-\gamma-\delta/2)}{\rho} - 1\right]e^{\epsilon-\gamma-\delta/2} - \frac{4n\pi(\epsilon-\gamma-\delta/2)}{\rho^4}$$

$$n = 1,2,\ldots \qquad \rho = \left[n^2\pi^2 + \left(\epsilon-\gamma-\frac{\delta}{2}\right)^2\right]^{1/2}$$

$$I_{26} = -\frac{1}{\beta}\left[I_{16} + (1-\nu_0)\int_0^1 e^{(\epsilon-\delta/2)x}\sin(n\pi x)\,dx\right] \qquad n = 1,2,\ldots$$

I'_{ij} can be obtained from the corresponding I_{ij} by setting $\epsilon = 0$.

APPENDIX B

Kernel $K(r,s)$ in Eq. (38)

The kernel $K(r,s)$ in the singular integral equation (38) is

$$K(r,s) = \frac{a}{2b}\left\{\frac{\gamma}{2}e^{(\gamma/4)(a/b)(s-r)}E_i\left[-\left(\frac{\gamma}{4}\right)\left(\frac{a}{b}\right)(s-r)\right] - bk(r,s)\right\}$$

where

$$E_i(z) = 0.57722 + \ln|z| + \sum_{n=1}^{\infty}\frac{z^n}{nn!}$$

and $k(r,s)$ is a very complicated function that is not given here but can be obtained from the authors.